

Article

# Anticorrosion Performance of Magnesium Hydroxide Coatings on Steel Substrates

Domna Merachtsaki , Ilias Toliopoulos , Efrosini Peleka and Anastasios Zouboulis \* 

Division of Chemical and Environmental Technology, Department of Chemistry, Aristotle University of Thessaloniki, 54124 Thessaloniki, Greece

\* Correspondence: zoubouli@chem.auth.gr

**Abstract:** Sewerage systems consist of several different parts, components and materials. Many of them are metallic structures, such as pumps, valves, ladders and wells, which are necessary for the proper operation of wastewater transport systems. Wastewater pipelines can be a highly corrosive environment, mainly due to the presence of biogenic sulfuric acid. In the present study, seven magnesium hydroxide and one magnesium oxide materials were used as protective coatings applied onto the surface of certain stainless steel and mild steel specimens against sulfuric acid corrosion. The coated specimens were subjected to accelerated sulfuric acid spraying tests and their behavior was evaluated by using optical observation, mass measurements and electrochemical impedance spectroscopy. According to the results, the coating prepared from a magnesium hydroxide powder with relatively low specific surface area and smaller particle size was optimal for the protection of the examined steel specimens.

**Keywords:** corrosion control; magnesium hydroxide coatings; stainless steel; mild steel; electrochemical impedance spectroscopy



**Citation:** Merachtsaki, D.; Toliopoulos, I.; Peleka, E.; Zouboulis, A. Anticorrosion Performance of Magnesium Hydroxide Coatings on Steel Substrates. *Constr. Mater.* **2022**, *2*, 166–180. <https://doi.org/10.3390/constrmater2030012>

Received: 15 June 2022

Accepted: 3 August 2022

Published: 6 August 2022

**Publisher's Note:** MDPI stays neutral with regard to jurisdictional claims in published maps and institutional affiliations.



**Copyright:** © 2022 by the authors. Licensee MDPI, Basel, Switzerland. This article is an open access article distributed under the terms and conditions of the Creative Commons Attribution (CC BY) license (<https://creativecommons.org/licenses/by/4.0/>).

## 1. Introduction

Microbiologically induced corrosion (MIC) is mainly responsible for the extended corrosion of construction materials in most wastewater transport pipeline systems. The sewer infrastructure is constructed mainly of concrete (especially large diameter pipes) and steel (i.e., valves, pumps, ladders, small diameter pipes, etc.). MIC takes place when microorganisms, such as specific bacteria, excrete corrosive metabolic products to their environment [1,2]. More specifically, biogenic sulfuric acid can be produced from microorganisms (sulfur oxidizing bacteria), and when the acid contacts the relevant surfaces, this leads to the formation of corrosion products, which overall weaken the structural stability of the sewerage system.

In order to mitigate the corrosion problems, several methods are examined and used, such as the replacement of construction materials with corrosive-resistant ones [3,4], or the addition of specific chemicals to the wastewater (such as nitrates, nitrites or bases such as sodium hydroxide) to block the microorganisms' development [5,6]. Finally, the application of protective coatings on the surfaces is commonly applied as a cheaper solution, to avoid costly replacement or the supplementary contamination of wastewater with the added chemical agents. Several different anti-corrosion protective coatings have been studied for concrete [7,8] as well as for the protection of steel surfaces in the relevant literature [9,10]. Magnesium-based coatings have already been studied for the protection of concrete against the sulfuric acid attack, due to their ability to react with the acid (neutralizing it), as well as their alkaline characteristics (maintaining alkaline surface values), which create a hostile environment for the growth of unwanted bacteria [11–15].

Magnesium hydroxide coatings are environmentally safe, non-toxic and relatively low-cost, in contrast to polymeric coatings. In that way, they can be studied for the

protection of steel surfaces used in the sewer pipe system. Modified magnesium hydroxide coatings were applied on magnesium alloys and studied for their corrosion protection in a relevant study [16]. To our knowledge, no research has been performed evaluating magnesium hydroxide coatings for their corrosion protection on steel substrates under sulfuric acid attack.

In this study, magnesium hydroxide coatings were applied onto steel substrates and examined for their anticorrosion ability. The coatings were prepared by using magnesium hydroxide and/or oxide powders, with different properties (i.e., specific surface area and particle size distribution). Seven magnesium hydroxide coatings and one magnesium oxide coating were applied on the surface of specific stainless steel and mild steel specimens, materials commonly used in sewerage applications. After that, the coated steel specimens were subjected to accelerated acid spraying tests. The protection of the substrates was evaluated with optical observation, mass measurements and electrochemical impedance spectroscopy measurements (EIS).

## 2. Materials and Methods

### 2.1. Coatings and Substrates

#### 2.1.1. Coatings

Eight coatings were examined (C1–C8), seven based on magnesium hydroxide and one based on magnesium oxide. The magnesium oxide and hydroxide powders, used for the preparation of coatings, were supplied by Grecian Magnesite S.A. (Gerakini, Greece); their detailed chemical composition and properties were presented in previous relevant studies [12,14,17]. The magnesium hydroxide powders, used for coating purposes, result from the hydration of magnesium oxide powders having different properties (i.e., specific surface area, MgO content), and under different preparation conditions (i.e., duration of hydration, hydration agent).

The magnesium hydroxide powders presented different specific surface area, particle size distribution and purity, and we aimed to examine the different impacts of major physicochemical properties on the protection performance of each coating. The composition of the powders is presented in Table 1 and the respective specific surface areas and particle size distributions of these powders are presented in Table 2. The coatings were synthesized by the addition of deionized water and the respective solid powders. For the magnesium hydroxide coatings, methylcellulose was also added (0.4 wt %) to enhance the coatings' adhesion onto the surface of steel specimens, as well as a common dispersant polymer to improve the coatings' dispersion stability and workability. The respective synthesis route was extensively described previously [12,14].

The thickness of applied coatings ranged between 0.8 and 1.2 mm, and its selection was based on relevant literature and preliminary studies [14,18–20]. Preliminary studies also determined the amount of coating to be applied in order to obtain the desired thickness, being 0.18–0.20 g/cm<sup>2</sup>.

**Table 1.** Composition of the studied powders [17].

	MgO	SiO <sub>2</sub>	CaO	Fe <sub>2</sub> O <sub>3</sub>	Al <sub>2</sub> O <sub>3</sub>	SO <sub>3</sub>	LOI
C1	63.49	8.77	2.30	0.15	0.15	0.11	25.03
C2	63.15	8.73	2.29	0.15	0.15	0.11	25.42
C3	66.54	3.05	1.48	0.07	0.07	0.09	28.70
C4	61.91	8.80	2.31	0.15	0.15	0.11	26.57
C5	65.00	3.32	1.52	0.08	0.05	0.14	29.90
C6	62.81	4.25	2.46	0.25	0.10	0.02	30.11
C7	66.76	0.40	0.30	0.03	0.05	0.10	32.06
C8	82.34	11.70	3.07	0.20	0.20	0.15	2.34

**Table 2.** Specific surface area (SSA) and particle size distribution (PSD) of the studied powders [17].

Material	SSA (m <sup>2</sup> /g)	PSD (μm)	
		D <sub>50</sub>	D <sub>90</sub>
C1	13.1	17.8	69.1
C2	18.7	8.4	29.5
C3	11.2	10.5	39.9
C4	13.2	9.5	40.8
C5	32.3	9.9	38.1
C6	7.0	3.8	13.1
C7	16.6	6.0	25.5
C8	17.7	19.5	51.5

### 2.1.2. Substrates

The steel test specimens were selected as stainless steel 316 and hot-rolled mild steel, based on the relevant literature regarding common materials of use in relevant studies and in sewerage systems [21–23]. The specimens' dimensions were 4.8 cm × 1.5 cm × 0.2 cm. The edges of the specimens were smoothed by using a grinding wheel, so that the coatings can remain attached. After the specimens were washed with water, they were chemically cleaned with petroleum ether and acetone to remove fats and grease from their surfaces, which may hinder the proper coating application.

### 2.1.3. Coatings' Application onto Steel Substrate

The coatings were applied onto the steel specimens manually by using a spatula at the rate of 0.0018–0.002 g/mm<sup>2</sup>, according to relevant studies [12–14]. After that, the coatings were dried for 3 days under normal laboratory conditions, i.e., temperature 21 ± 2 °C and relative humidity 60 ± 10%, before testing. Although the solidification of magnesium oxide slurry was very fast, the respective coated specimens were dried for 3 days, along with the other coated specimens.

## 2.2. Sulfuric Acid Spraying Test

A laboratory-scale sulfuric acid spraying test was used to create accelerated corrosion conditions based on the conditions existing in the real sewer pipe environment. More specifically, a sulfuric acid solution (0.2 M) was used to simulate the biogenic sulfuric acid that is produced by microorganisms during MIC. The respective test was empirically developed, based on the standard salt spray test [24,25]. The sulfuric acid was sprayed in the specifically designed chamber to form a corrosive mist, which then could contact the coated and uncoated steel specimens. A custom-made poly (methyl methacrylate) chamber (Figure 1) was used, designed with specimen support slots and equipped with proper nebulizers. A condensate drain was also designed for the removal of rinse solution.

The selected spraying process duration was 4 days [14]. Every day, three specimens were removed from the chamber and subjected to subsequent mass and EIS measurements.



**Figure 1.** Custom-made spraying chamber with nebulizers and adjusted coated metallic specimens.

### 2.3. Evaluation Methods

#### 2.3.1. Mass Measurements

The mass change of materials is a common corrosion evaluation method since both the formation of by-products and the loss of material can be measured. In this study, the specimens' mass was recorded before applying the coatings and before the acid spraying test (denoted as the initial mass). At the end of acid spraying test, the coatings' mass was recorded again (denoted as final mass). After the acid spraying test, the specimens were cleaned by scrubbing with a brush, so that the coating and the rust were removed. The initial and the final mass were used to calculate the overall mass change, aiming to evaluate the corrosion degree. An electronic balance (Kern PCB 350-3, Kern-Sohn GmbH, Balingen, Germany) was used for the mass recordings.

#### 2.3.2. Electrochemical Impedance Spectroscopy (EIS)

Electrochemical Impedance Spectroscopy was used for the examination of corrosion regarding the coated and uncoated metallic specimens. According to the relevant literature [10,16,26] and the basic principles of EIS, this method can be used to evaluate the corrosion degree of (mostly metallic) systems, and consequently, can help to evaluate the coatings' protection ability.

The impedance measurements were performed by using a Vertex One potentiostat (Ivium Technologies, Eindhoven, Netherlands) and the results were recorded by the respective software (IviumSoft, Ivium Technologies, Eindhoven, Netherlands). A three-electrode cell was used (Figure 2), applying the  $\text{KNO}_3$  solution (0.5 M) as an electrolyte, an Ag/AgCl reference electrode and a Pt sheet counter-electrode; finally, the steel specimens were used as working electrodes. A sulfuric acid solution was not used as an electrolyte during the EIS measurements; it was replaced by a  $\text{KNO}_3$  solution, aiming to evaluate the corrosion degree of the performed acid spraying test, but not provoking any additional reaction/corrosion.

The measurements were conducted at the open circuit potential (OCP) by applying a sinusoidal voltage signal of 10 mV, with the frequency ranging from  $10^5$  Hz to  $10^{-2}$  Hz and 10 measurement points per decade. Each experiment was repeated at least twice and carried out on the specimens after 1, 2, 3 and 4 days of acid spraying tests. The experimental data were fitted with suitable equivalent circuits by using ZsimpWin software.

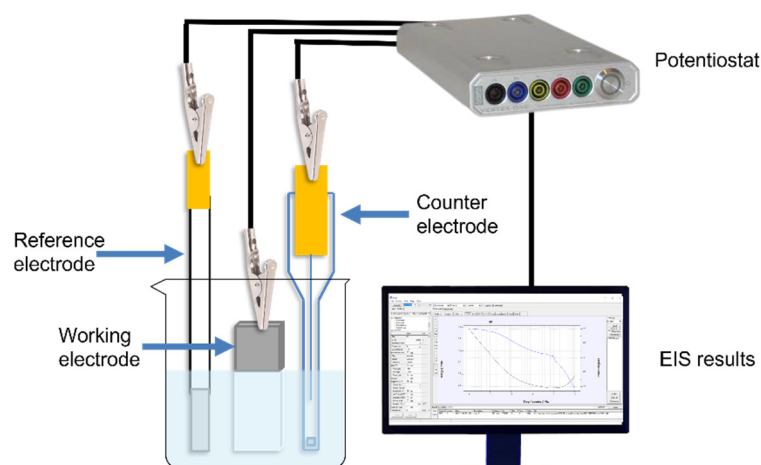


**Figure 2.** The 3-electrode cell and the experimental set-up of the electrochemical impedance spectroscopy measurements.

### 3. Results

#### 3.1. Optical Observation

The coated and uncoated steel specimens were optically observed for rust formation on their surfaces, indicating the oxidation/corrosion of steel. As a result, the specimens presenting extended rust formation showed that the examined coatings could not protect the steel substrate. However, several studied coatings seemed to sufficiently protect the surface of steel, mostly in the case of mild steel specimens. In the case of stainless steel specimens, no extended corrosion was optically observed, because stainless steel is generally difficult to corrode, and therefore, it was not easy to come up with safe conclusions through the optical observation only.

Figure 3 presents the coated and uncoated stainless steel specimens after 4 days of acid spraying. More precisely, the coated specimens are presented after the removal of used coatings to examine their surface for possible rust formation. However, no rust was noticed to be formed on both coated and uncoated stainless steel specimens, so it is not clear through the optical observation only whether the coatings can offer any protection to these substrates. Stainless steel 316 is an alloy containing 16.5–18.5% of chromium, in contrast to mild steel, which contains a maximum of 1% chromium. Chromium forms a protective layer on the steel surface due to its reaction with oxygen, which is responsible for the specific anticorrosion properties of stainless steel. However, under extreme and severe corrosive conditions, this layer can collapse, thus still allowing the corrosion of steel substrate.

In the case of mild steel specimens, the coatings' protection can be optically observed. Figure 4a shows the uncoated steel specimen after 4 days of acid spraying; the rust formation is obvious. In contrast, Figure 4b,c show the specimens' surface after removing the coatings C6 and C5, respectively. In these cases, the specimens seemed to be sufficiently protected from corrosion. However, some coatings could not equally protect the respective metal substrate, as it was observed for the specimens with coatings C2 and C4.

Additionally, an optical microscope was used to examine in detail selected steel surfaces, both of coated and uncoated specimens. The images are presented in the Supplementary Materials (Figures S1 and S2). These observations confirmed that the uncoated mild steel specimens presented severe corrosion after the acid spraying test, in contrast to the stainless steel specimens. Moreover, it was noticed that even for the stainless steel specimens coated with the C2 sample (i.e., presenting relatively lower corrosion protection), some spots of rust were observed, in contrast to the specimens coated with the C6 sample, which did not present any corrosion spots.

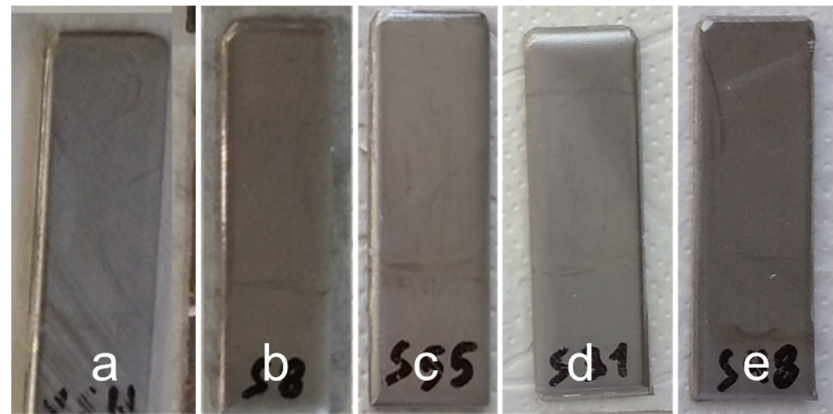


**Figure 3.** Comparing selected representative coated (after removing the coating) and uncoated stainless steel specimens after 4 days of acid spraying tests: (a) uncoated specimen, (b) coated specimen with C6 coating, (c) coated specimen with C5 coating, (d) coated specimen with coating C2, (e) coated specimen with C4 coating.

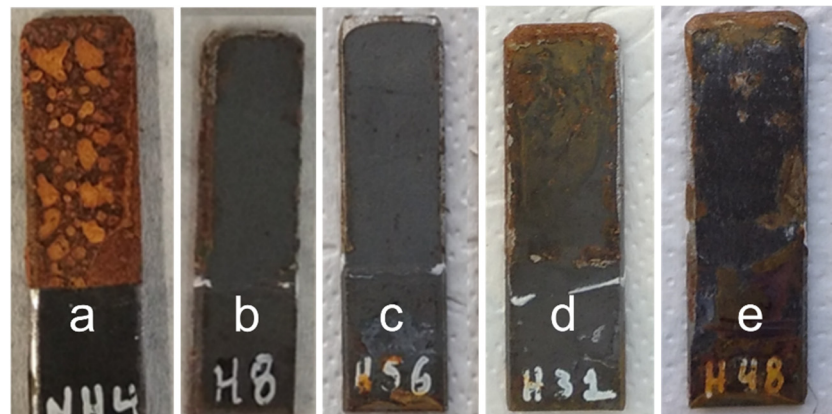


**Figure 4.** Comparing selected representative coated (after removing the coating) and uncoated mild steel specimens after 4 days of acid spraying tests: (a) uncoated specimen, (b) coated specimen with C6 coating, (c) coated specimen with C5 coating, (d) coated specimen with coating C2, (e) coated specimen with C4 coating.

### 3.2. Mass Measurements

The mass results are presented with respect to the specimens' mass, before and after the acid spraying test. Coated and uncoated specimens were cleaned, so that rust and coatings were removed. The extent of corrosion was estimated by comparing the initial and final mass of specimens.

As it was concluded through the optical observation, the coated and uncoated stainless steel specimens did not present any corrosion. This fact was also obvious through the respective mass measurements, as in all cases, the mass of specimens remained constant (Figure 5) during the acid spraying test. For this reason, in these cases, no conclusions could be positively drawn regarding the protection of stainless steel specimens by applying the examined coatings.

However, in the case of coated and uncoated mild steel specimens (Figure 6), the mass results were different when comparing with the stainless steel specimens, as the relevant optical observations were also different. The uncoated specimens were badly corroded, and the specimens' mass was reduced by at least 1% with respect to the initial mass. On the contrary, the examined coatings seemed to sufficiently protect the substrates, as the mass of coated mild steel specimens remained constant in most cases. Specimens coated with coating C4 presented a small mass reduction ( $\sim 0.4\%$ ), which indicated the reduced protection given by this specific coating.

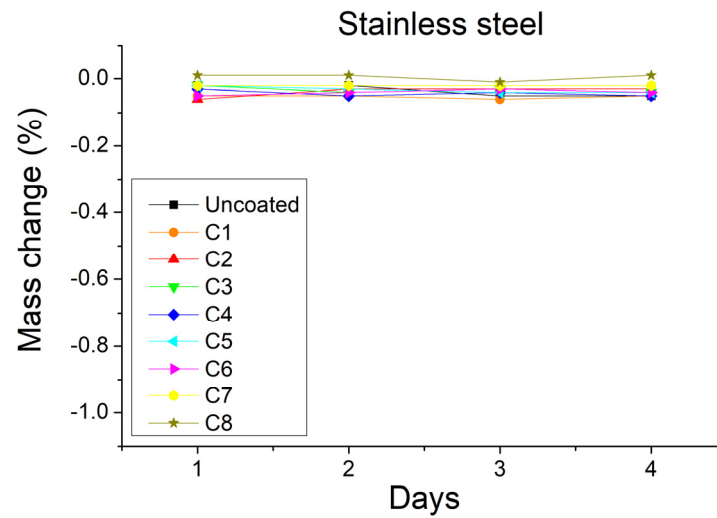


Figure 5. Mass change of coated and uncoated stainless steel specimens during the acid spraying tests.

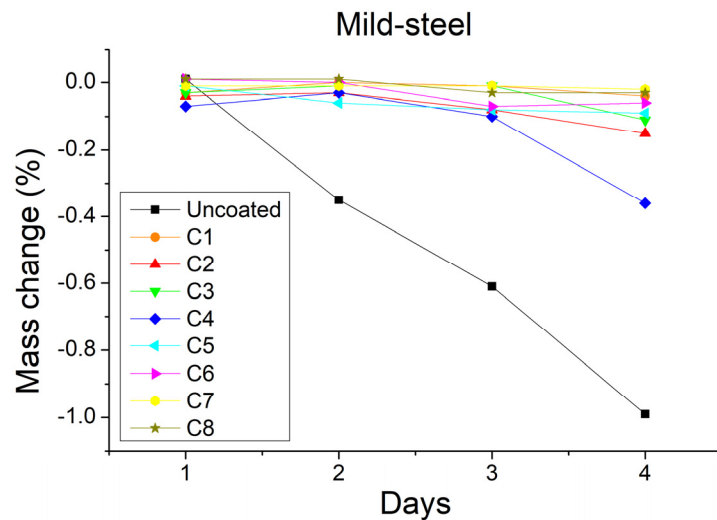
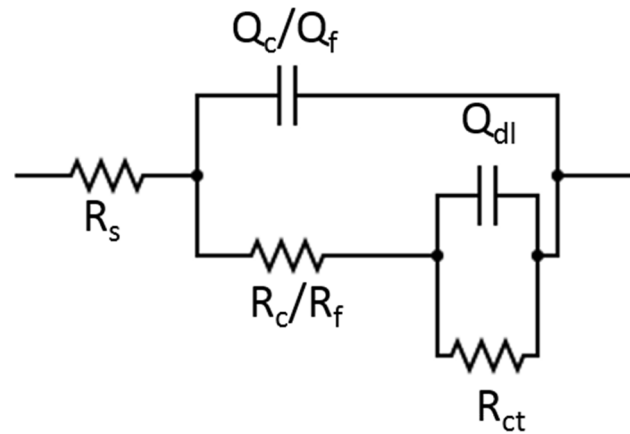


Figure 6. Mass change of coated and uncoated hot-rolled mild steel specimens during the acid spraying tests.

### 3.3. Electrochemical Impedance Spectroscopy

The fitting of the impedance results was performed by using the equivalent circuit of Figure 7. Several equivalent circuits can be used, aiming to better describe each system. The EIS is used to draw useful and practical conclusions for the studied system, so the spectrum simulations based on more complicated equivalent circuits are not expected to offer any better practical information. The respective equivalent circuit was selected according to the relative literature [10,21,27,28], and the reliability of respective fitting was confirmed by the chi-squared values, being in the order of  $10^{-3}$  or smaller in most cases.

The basic parameters of this equivalent circuit for the coated and uncoated specimens are the solution resistance ( $R_s$ ), the double layer admittance ( $Q_{dl}$ ), and the charge transfer resistance ( $R_{ct}$ ). The other parameters differ for the coated and uncoated specimens. More precisely, for the coated specimens, the coating resistance ( $R_c$ ) and the coating constant phase element ( $Q_c$ ) were used, whereas for the uncoated specimens, the resistance of corrosion products ( $R_f$ ) and the double layer capacitance at the corrosion products/solution interface ( $Q_f$ ) were used [29].



**Figure 7.** The simple electrical equivalent circuit used to fit the EIS data for the coated and uncoated steel specimens.

Figures 8 and 9 show the impedance spectra (Nyquist plots) that resulted for the coated and uncoated steel specimens after 4 days of acid spraying tests. The results of the EIS measurements were single results, selected to represent the relevant spectra between the two outliers of the three specimens, tested for each type of sample. Figure 8 shows the results for the stainless steel specimens and Figure 9, the mild steel specimens. The data points correspond to the experimental data and the solid lines represent the fitting values. The obtained data were very well fitted, according to these figures. It can also be concluded that some coatings increased the total resistance, and as a result, they seemed to better protect the substrates.

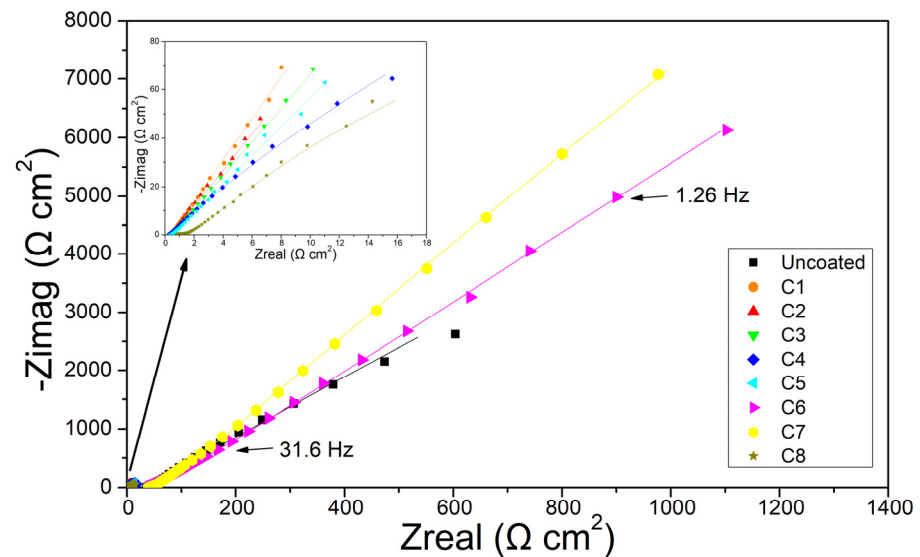


**Figure 8.** Nyquist plot of coated and uncoated stainless steel specimens after 4 days of acid spraying tests; the points indicate experimental data, and the lines indicate the fitting of these data by using the equivalent circuit of Figure 7.

Bode plots are presented in Figures 10 and 11 for stainless and mild steel specimens, respectively. The increased phase angle of coated specimens, compared to uncoated ones, indicated the protection provided from the coatings against corrosion [10]. Considering the bode plot of  $|Z|$  vs.  $\log$  frequency, a decrease at lower frequencies (where the corrosion charge transfer process prevails) was observed, while values were aligned with the x-axis at higher frequencies in all cases. The higher values of impedance modulus

at lower frequencies for the specimens coated with coatings C6 and C7 indicated higher corrosion protection.

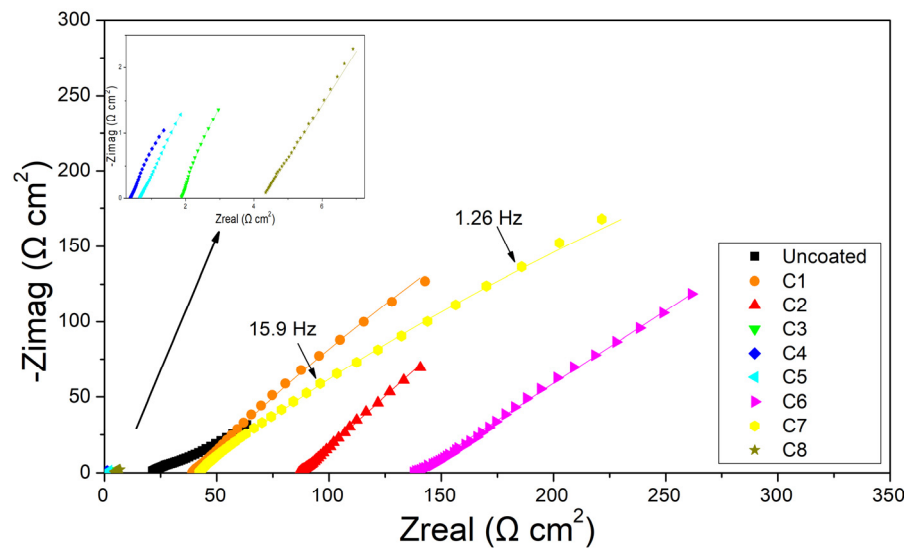


**Figure 9.** Nyquist plot of coated and uncoated hot-rolled mild steel specimens after 4 days of acid spraying tests; the points indicate the experimental data, and the lines indicate the fitting of these data by using the equivalent circuit of Figure 7.

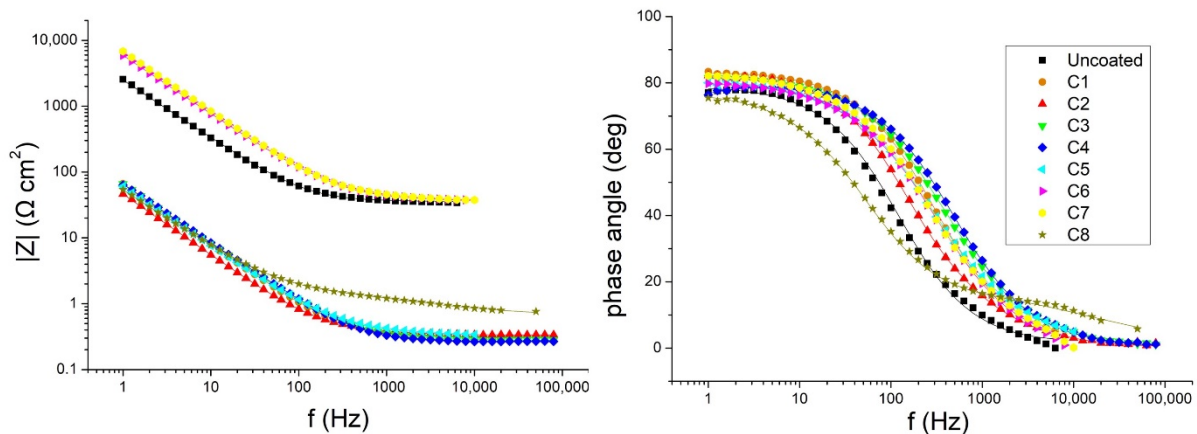


**Figure 10.** Bode plots of coated and uncoated stainless steel specimens after 4 days of sulfuric acid spraying tests; the points indicate the respective experimental data, and the lines indicate the fitting of these data by using the equivalent circuit of Figure 7. **Left:**  $|Z|$  vs. log frequency, **right:** phase angle vs. log frequency.

The differences in Bode curves between specimens are larger in the case of mild steel, according to Figure 11. Some coated mild steel specimens presented higher impedance at low-frequency values than the uncoated specimens, indicating better corrosion protection [16]. In both Bode diagrams (i.e., stainless steel and mild steel), the maximum angles are lower than  $90^\circ$ , indicating that the systems did not behave as ideal capacitors [30]; this is also in line with the  $n$  values of the CPE corresponding to the surface film (significantly lower than 1).

In order to draw more accurate conclusions, the respective parameters values should be examined more closely.

The parameters resulting by the fitting of experimental data were estimated and presented in the Supplementary Materials (see Tables S1–S18). These parameters offer a deeper understanding of the system, and they were used to evaluate the coating’s protection

ability. More specifically, the charge transfer resistance ( $R_{ct}$ ) is the main parameter that is commonly examined when metal corrosion is studied [10,16,27,31].

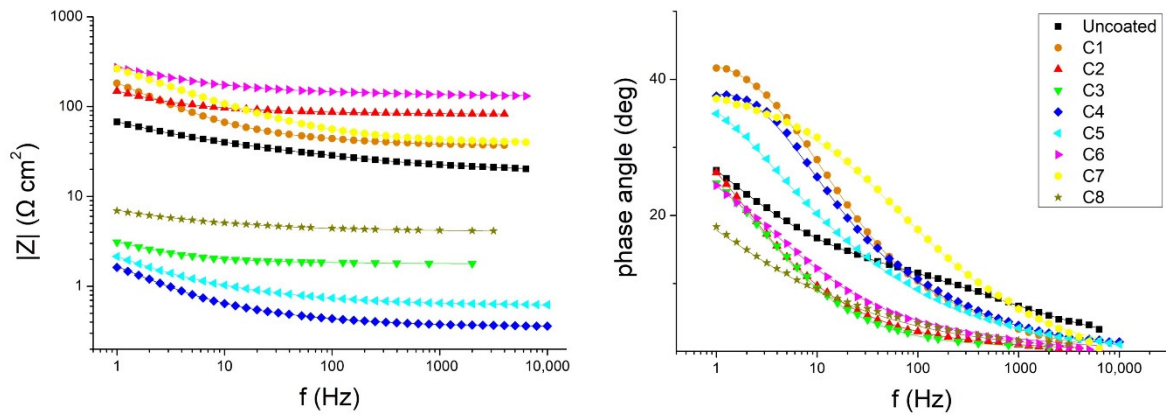


**Figure 11.** Bode plots of coated and uncoated hot-rolled mild steel specimens after 4 days of sulfuric acid spraying tests; the points indicate the respective experimental data, and the lines indicate the fitting of these data by using the equivalent circuit of Figure 7. **Left:**  $|Z|$  vs. log frequency, **right:** phase angle vs. log frequency.

Figures 12 and 13 present the charge transfer resistance for the coated and uncoated specimens of stainless steel and mild steel, respectively. According to Figure 12, the uncoated stainless steel specimens presented relatively stable resistance during the 4 days of acid spraying tests, indicating that the specimens were not corroded, maintaining their resistance. However, in some cases, the coated specimens presented larger  $R_{ct}$  values than the uncoated ones; hence, they block the electron transfer to the steel surface. As an example, the coated stainless steel specimens with the coating C6 maintain higher  $R_{ct}$  values during the test than the uncoated specimens. Moreover, specimens coated with certain coatings, such as C1, C2, C4 and C7, were found to present higher  $R_{ct}$  values during the first days of the acid spraying test, but a decrease was observed at the end of this test, indicating possible coating defects or consumption that reduced the resistance, and therefore also the protection.

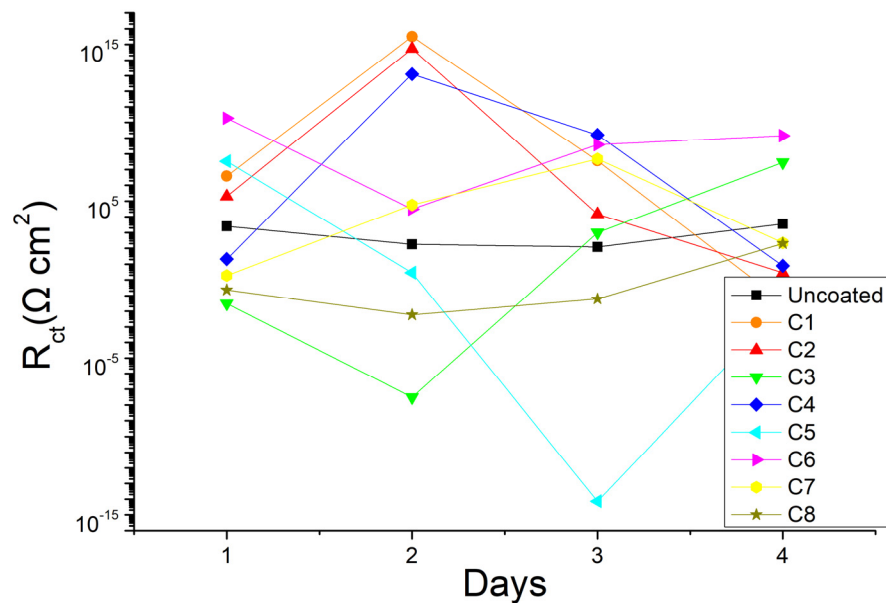


**Figure 12.** Charge transfer resistance ( $R_{ct}$ ) of coated and uncoated stainless steel specimens, resulting from the fitting of relevant data.

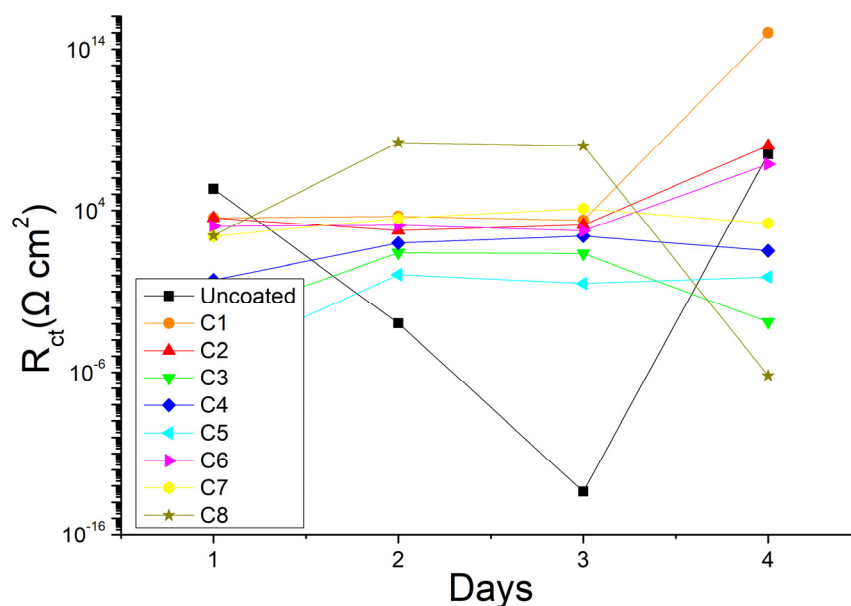


**Figure 13.** Charge transfer resistance ( $R_{ct}$ ) of coated and uncoated hot-rolled mild steel specimens resulting from the fitting of relevant data.

The initial  $R_{ct}$  values of uncoated mild steel specimens were found to be reduced by the time of acid spray test, as the test proceeds (Figure 13). This fact indicates the constant corrosion of specimens due to the reaction of steel with sulfuric acid. However, on the 4th day, the value of this parameter was increased again, reaching the initial values. This phenomenon was due to the extended formation of corrosion products on the specimens’ surface, according to the relevant literature [32]. The coated specimens with coating C8 presented increased  $R_{ct}$  values during the initial days of the spraying test, but these values were decreased at the 4th day, indicating the detachment of the coating or the fast consumption of it. The coatings C1, C2 and C6 seemed to maintain high  $R_{ct}$  values by the end of the test, and hence seemed to effectively protect the substrate.

#### 4. Discussion

Magnesium hydroxide and oxide coatings were previously studied as concrete protective coatings against biogenic sulfuric acid corrosion, and the effect of the raw materials’ characteristics (e.g., purity, specific surface area, particle size distribution) on the coatings’ corrosion protection ability was previously defined [12,13,17]. Accordingly, in this study, the same coatings were applied on two different steel specimens, evaluating their corrosion protection performance, because apart from concrete, steel surfaces are also used in sewerage network environments and subjected to corrosion. These coatings can react/neutralize sulfuric acid and preserve alkaline surface pH, which are considered important properties that can block the development of microorganisms producing biogenic sulfuric acid in sewer systems.

According to the obtained results, the stainless steel specimens seemed to inhibit corrosion by themselves, as it was expected for this type of steel. No optical defects were observed, and no rust (i.e., the main corrosion by-product) was noticed to be formed. These optical observation results were confirmed also by the relevant mass measurements, as no mass change was recorded, both for uncoated and coated specimens of this steel type. However, the EIS measurements revealed that some coated specimens, such as the specimens coated with coatings C6 and C3, presented increased charge transfer resistance ( $R_{ct}$ ); hence, these coatings can protect even the stainless steel surfaces over time. This improvement of  $R_{ct}$  values is comparable with other protective coatings, such as silane-based coatings, previously studied by Ziadi et al. [10], which also seemed to enhance the  $R_{ct}$  values of stainless steel 304, even though the later specimens were tested in urban wastewater (as the

corrosive environment) and not by harsh sulfuric acid spraying as in this study. Additionally, the respective values are higher than the values of specific chemically reactive enamel coated steel bar specimens presented in another relevant study [28]. Moreover, some coated stainless steel specimens presented a large drop in the  $R_{ct}$  value, such as specimens coated with coatings C1, C2 and C3, indicating extended degradation and limited protection. Similar behavior was observed in a relevant study for epoxy-amine urethane coatings when applied onto mild steel specimens [9].

On the contrary, the optical observations for the uncoated mild steel specimens showed that the corrosion caused by sulfuric acid was extended and this can lead to severe rust formation. However, the coated mild steel specimens presented very good protection results against corrosion, as in most cases, the protected specimens were either not corroded, or only some specific corroded spots were observed. The coatings react with the sprayed sulfuric acid, neutralizing it, and can effectively protect the steel surface against acid corrosion. However, the respective optical observations showed that not all coatings presented equally effective protection results, as some of them allowed the penetration of acid, due to defects or fast consumption/interaction with the sprayed sulfuric acid. For example, the coatings C2 and C4 presented the worst behavior among all examined coatings regarding the corrosion protection. However, other coatings, such as C6 and C5, offered satisfactory protection for the mild steel substrates, as no corrosion was optically observed. Mass measurements agreed with these observations, as the mild steel specimens coated with the coating C4 presented the largest mass reduction (except for the uncoated specimens), followed by those coated with the C2 coating. The other coatings presented almost zero mass change, indicating very good corrosion protection. The respective EIS results indicated that the coatings C1, C2 and C6 increased the charge transfer resistance of steel specimens, and as a result, can offer better protection. On the contrary, there is only one case between the examined coated specimens found to present several orders of  $R_{ct}$  value reduction, i.e., the specimens coated with coating C8. Other coated specimens, such as those with coatings C3 and C7, presented smaller reductions in  $R_{ct}$  values. In comparison to other polymeric coatings, and according to relevant studies [9], some magnesium hydroxide coatings can offer better protection to mild steel substrates, as they present increased  $R_{ct}$  values (e.g.,  $10^{14} \Omega \text{ cm}^2$  in the case of C1 coating).

The equivalent circuit used in the present study was also previously used in other relative literature studies regarding the use of coatings for the protection of metal substrates and was examined in different corrosive environments. Ziadi et al. [10] used the same equivalent circuit for the study of silane-based coatings, whereas Wu et al. [16] used this circuit for the fitting of experimental data, regarding coated magnesium alloys with magnesium hydroxide coating. In all cases, the charge transfer resistance of bare metallic surfaces was smaller with respect to the coated metallic specimens, indicating that sufficient protection was offered by these coatings to the metal substrates.

According to the obtained results, the coating C6 seemed to present the optimal protection for both examined types of steel. Other coatings can also efficiently protect the substrates, i.e., coating C3 for stainless steel and coatings C1 and C2 for mild steel specimens, but coating C6 can protect both metallic substrates. This coating was also found to be among the optimal selections for the protection of concrete against acid corrosion, according to the relevant literature [17]. The low specific surface area ( $7 \text{ m}^2/\text{g}$ ) and the smaller particle size ( $d_{90} = 13.1 \mu\text{m}$ ) of this material, when comparing to the other studied materials, seemed to enhance its performance regarding the protection of steel surfaces from sulfuric acid corrosion.

The results of this study showed that the magnesium hydroxide and/or oxide powders can be effectively used as coatings for the corrosion protection of steel surfaces in sewerage systems. In that way, the degradation of metallic surfaces subjected to biogenic sulfuric acid attack can be prevented, hence preserving the structure and avoiding equipment damage. Therefore, these materials can be applied throughout the pipeline network—both to the

concrete pipes, according to previous studies [13,14], as well as the steel surfaces (such as pumps, ladder, valves, etc.).

Future studies regarding magnesium hydroxide coatings for steel surfaces protection can focus on testing these materials under real sewer conditions, or in the presence of microorganisms. Moreover, other electrochemical methods, such as the Tafel method or cyclic polarization [29,33], can also be used to examine the anticorrosion properties of these coatings when applied on different steel surfaces.

## 5. Conclusions

Magnesium hydroxide and magnesium oxide coatings were used as protective coatings and were applied on stainless steel and mild steel specimens. These coatings were examined for their protection against sulfuric acid corrosion so that they can be applied on steel surfaces in sewer environments where biogenic sulfuric acid is considered the main corrosive agent.

The optical observations and the mass measurements showed that the stainless steel remained unharmed, both coated and uncoated, as no corrosion and no mass change were observed. In contrast, the mild steel specimens seemed to be effectively protected from corrosion by the application of the respective coatings. The uncoated mild steel specimens were corroded after the sulfuric acid spraying test, based on the optical observations and the resulting mass changes/reduction. On the contrary, no corrosion was optically observed for the coated mild steel specimens, and they presented almost zero mass change, indicating that most coatings can effectively protect the mild steel substrate.

The electrochemical impedance measurements showed that some coatings enhance the charge transfer resistance of the specimens, hence better protecting the metal substrates from corrosion. In the case of stainless steel substrates, the coatings C6 and C3 presented increased resistance, while in the case of mild steel specimens, the coatings C1, C2 and C6 maintained increased resistance after the end of acid spraying test.

The coating C6 is the optimal coating that can produce satisfactory results for both type of steels, better protecting the metal/steel substrates for a longer duration.

**Supplementary Materials:** The following supporting information can be downloaded at: <https://www.mdpi.com/article/10.3390/constrmater2030012/s1>, Figure S1: Surface observations, by using an optical microscope, of uncoated stainless steel specimens (a) before and (b) after 4 days of acid spraying test, and of uncoated mild steel specimens (c) before and (d) after 4 days of acid spraying test. Figure S2: Surface observations, by using an optical microscope, of coated stainless steel specimens with coating (a) C6 and (b) C2 the acid spraying test, and of coated mild steel specimens with coating (c) C6 and (d) C2, after 4 days of acid spraying test and after removing the coatings. Table S1: Parameter values of the equivalent circuit that result from the fitting of the experimental data of the uncoated stainless steel specimens; Table S2: Parameter values of the equivalent circuit that result from the fitting of the experimental data of the coated stainless steel specimens with coating C1; Table S3: Parameter values of the equivalent circuit that result from the fitting of the experimental data of the coated stainless steel specimens with coating C2; Table S4: Parameter values of the equivalent circuit that result from the fitting of the experimental data of the coated stainless steel specimens with coating C3; Table S5: Parameter values of the equivalent circuit that result from the fitting of the experimental data of the coated stainless steel specimens with coating C4; Table S6: Parameter values of the equivalent circuit that result from the fitting of the experimental data of the coated stainless steel specimens with coating C5; Table S7: Parameter values of the equivalent circuit that result from the fitting of the experimental data of the coated stainless steel specimens with coating C6; Table S8: Parameter values of the equivalent circuit that result from the fitting of the experimental data of the coated stainless steel specimens with coating C7; Table S9: Parameter values of the equivalent circuit that result from the fitting of the experimental data of the coated stainless steel specimens with coating C8; Table S10: Parameter values of the equivalent circuit that result from the fitting of the experimental data of the uncoated mild steel specimens; Table S11: Parameter values of the equivalent circuit that result from the fitting of the experimental data of the coated mild steel specimens with coating C1; Table S12: Parameter values of the equivalent circuit that

result from the fitting of the experimental data of the coated mild steel specimens with coating C2; Table S13: Parameter values of the equivalent circuit that result from the fitting of the experimental data of the coated mild steel specimens with coating C3; Table S14: Parameter values of the equivalent circuit that result from the fitting of the experimental data of the coated mild steel specimens with coating C4; Table S15: Parameter values of the equivalent circuit that result from the fitting of the experimental data of the coated mild steel specimens with coating C5; Table S16: Parameter values of the equivalent circuit that result from the fitting of the experimental data of the coated mild steel specimens with coating C6; Table S17: Parameter values of the equivalent circuit that result from the fitting of the experimental data of the coated mild steel specimens with coating C7; Table S18: Parameter values of the equivalent circuit that result from the fitting of the experimental data of the coated mild steel specimens with coating C8.

**Author Contributions:** Conceptualization, E.P. and A.Z.; methodology, D.M.; validation, D.M.; investigation, D.M. and I.T.; resources, E.P. and A.Z.; data curation, D.M. and I.T.; writing—original draft preparation, D.M. and I.T.; writing—review and editing, E.P. and A.Z.; supervision, E.P. and A.Z.; project administration, E.P. and A.Z. All authors have read and agreed to the published version of the manuscript.

**Funding:** This research was co-financed by the European Union and Greek national funds through the Operational Program Competitiveness, Entrepreneurship and Innovation, under the call RESEARCH-CREATE-INNOVATE (project code: T1EDK-02355).

**Data Availability Statement:** The data presented in this study are available upon request from the corresponding author.

**Acknowledgments:** The authors wish to thank the Grecian Magnesite S.A. Company for supplying the raw materials and the respective information. The authors also wish to thank Sotiris Sotiropoulos for helpful discussions regarding EIS experiments.

**Conflicts of Interest:** The authors declare no conflict of interest.

## References

1. Usher, K.M.; Kaksonen, A.H.; Cole, I.; Marney, D. Critical Review: Microbially Influenced Corrosion of Buried Carbon Steel Pipes. *Int. Biodeterior. Biodegrad.* **2014**, *93*, 84–106. [[CrossRef](#)]
2. Foorginezhad, S.; Mohseni-Dargah, M.; Firoozirad, K.; Aryai, V.; Razmjou, A.; Abbassi, R.; Garaniya, V.; Beheshti, A.; Asadnia, M. Recent Advances in Sensing and Assessment of Corrosion in Sewage Pipelines. *Process Saf. Environ. Prot.* **2021**, *147*, 192–213. [[CrossRef](#)]
3. Justo-Reinoso, I.; Hernandez, M.T. Use of Sustainable Antimicrobial Aggregates for the In-Situ Inhibition of Biogenic Corrosion on Concrete Sewer Pipes. *MRS Adv.* **2019**, *4*, 2939–2949. [[CrossRef](#)]
4. Chetty, K.; Xie, S.; Song, Y.; McCarthy, T.; Garbe, U.; Li, X.; Jiang, G. Self-Healing Bioconcrete Based on Non-Axenic Granules: A Potential Solution for Concrete Wastewater Infrastructure. *J. Water Process Eng.* **2021**, *42*, 102139. [[CrossRef](#)]
5. Cabral, L.L.B.; Sousa, J.T.; Lopes, W.S.; Leite, V.D.; Barbosa, R.A. Performance of Anaerobic Hybrid Reactor with Post-Treatment in Intermittent Flow Sand Filter: A Sulfide-Oxidizing Bioprocess for the Treatment of Sanitary Sewage Using Nitrate as Electron Acceptor. *Environ. Processes* **2020**, *7*, 1095–1109. [[CrossRef](#)]
6. Zhao, Z.; Yang, J.; Zhang, Z.; Wang, S.; Zhang, Z.; Lu, J. New Method for Efficient Control of Hydrogen Sulfide and Methane in Gravity Sewers: Combination of NaOH and Nitrite. *Front. Environ. Sci. Eng.* **2021**, *16*, 75. [[CrossRef](#)]
7. Wang, T.; Wu, K.; Kan, L.; Wu, M. Current Understanding on Microbiologically Induced Corrosion of Concrete in Sewer Structures: A Review of the Evaluation Methods and Mitigation Measures. *Constr. Build. Mater.* **2020**, *247*, 118539. [[CrossRef](#)]
8. Kong, L.; Fang, J.; Zhang, B. Effectiveness of Surface Coatings Against Intensified Sewage Corrosion of Concrete. *J. Wuhan Univ. Technol. Mater. Sci. Ed.* **2019**, *34*, 1177–1186. [[CrossRef](#)]
9. Potvin, E.; Brossard, L.; Larochelle, G. Corrosion Protective Performances of Commercial Low-VOC Epoxy/Urethane Coatings on Hot-Rolled 1010 Mild Steel. *Prog. Org. Coat.* **1997**, *31*, 363–373. [[CrossRef](#)]
10. Ziadi, I.; Alves, M.M.; Taryba, M.; El-Bassi, L.; Hassairi, H.; Boussemi, L.; Montemor, M.F.; Akrouit, H. Microbiologically Influenced Corrosion Mechanism of 304L Stainless Steel in Treated Urban Wastewater and Protective Effect of Silane-TiO<sub>2</sub> Coating. *Bioelectrochemistry* **2020**, *132*, 107413. [[CrossRef](#)]
11. Chatzis, A.; Merachtsaki, D.; Zouboulis, A. Performance of Three Magnesium-Based Coatings for Corrosion Protection of Concrete against Sulfuric Acid. *Environ. Processes* **2022**, *9*, 12. [[CrossRef](#)]
12. Merachtsaki, D.; Tsardaka, E.-C.; Anastasiou, E.; Zouboulis, A. Anti-Corrosion Properties of Magnesium Oxide/Magnesium Hydroxide Coatings for Application on Concrete Surfaces (Sewerage Network Pipes). *Constr. Build. Mater.* **2021**, *312*, 125441. [[CrossRef](#)]

13. Merachtsaki, D.; Tsardaka, E.-C.; Anastasiou, E.; Zouboulis, A. Evaluation of the Protection Ability of a Magnesium Hydroxide Coating against the Bio-Corrosion of Concrete Sewer Pipes, by Using Short and Long Duration Accelerated Acid Spraying Tests. *Materials* **2021**, *14*, 4897. [[CrossRef](#)] [[PubMed](#)]
14. Merachtsaki, D.; Tsardaka, E.-C.; Anastasiou, E.K.; Yiannoulakis, H.; Zouboulis, A. Comparison of Different Magnesium Hydroxide Coatings Applied on Concrete Substrates (Sewer Pipes) for Protection against Bio-Corrosion. *Water* **2021**, *13*, 1227. [[CrossRef](#)]
15. Sydney, R.; Esfandi, E.; Surapaneni, S. Control Concrete Sewer Corrosion via the Crown Spray Process. *Water Environ. Res.* **1996**, *68*, 338–347. [[CrossRef](#)]
16. Wu, W.; Zhang, F.; Li, Y.; Song, L.; Jiang, D.; Zeng, R.C.; Tjong, S.C.; Chen, D.C. Corrosion Resistance of Dodecanethiol-Modified Magnesium Hydroxide Coating on AZ31 Magnesium Alloy. *Appl. Phys. A Mater. Sci. Processing* **2020**, *126*, 8. [[CrossRef](#)]
17. Merachtsaki, D.; Tsiaras, S.; Peleka, E.; Zouboulis, A. Selection of Magnesium Hydroxide Coatings for Corrosion Mitigation in Concrete Sewer Pipes by Using Multiple Criteria Decision Analysis. *Environ. Sustain. Indic.* **2022**, *13*, 100168. [[CrossRef](#)]
18. Berndt, M.L. Evaluation of Coatings, Mortars and Mix Design for Protection of Concrete against Sulphur Oxidising Bacteria. *Constr. Build. Mater.* **2011**, *25*, 3893–3902. [[CrossRef](#)]
19. Diamanti, M.V.; Brenna, A.; Bolzoni, F.; Berra, M.; Pastore, T.; Ormellese, M. Effect of Polymer Modified Cementitious Coatings on Water and Chloride Permeability in Concrete. *Constr. Build. Mater.* **2013**, *49*, 720–728. [[CrossRef](#)]
20. Merachtsaki, D.; Fytianos, G.; Papastergiadis, E.; Samaras, P.; Yiannoulakis, H.; Zouboulis, A. Properties and Performance of Novel Mg(OH)<sub>2</sub>-Based Coatings for Corrosion Mitigation in Concrete Sewer Pipes. *Materials* **2020**, *13*, 5291. [[CrossRef](#)]
21. Kartsonakis, I.A.; Charitidis, C.A. Corrosion Protection Evaluation of Mild Steel: The Role of Hybrid Materials Loaded with Inhibitors. *Appl. Sci.* **2020**, *10*, 6594. [[CrossRef](#)]
22. Liu, C.; Bi, Q.; Matthews, A. EIS Comparison on Corrosion Performance of PVD TiN and CrN Coated Mild Steel in 0.5 N NaCl Aqueous Solution. *Corros. Sci.* **2001**, *43*, 1953–1961. [[CrossRef](#)]
23. Mansfeld, F. Electrochemical Impedance Spectroscopy (EIS) as a New Tool for Investigating Methods of Corrosion Protection. *Electrochim. Acta* **1990**, *35*, 1533–1544. [[CrossRef](#)]
24. ASTM B117-11; Standard Practice for Operating Salt Spray (Fog) Apparatus. ASTM International: West Conshohocken, PA, USA, 2011.
25. ASTM G85-11; Standard Practice for Modified Salt Spray (Fog) Test. ASTM International: West Conshohocken, PA, USA, 2011.
26. Hernández, H.H.; Reynoso, A.M.R.; González, J.C.T.; Morán, C.O.G.; Hernández, J.G.M.; Ruiz, A.M.; Hernández, J.M.; Cruz, R.O. Electrochemical Impedance Spectroscopy (EIS): A Review Study of Basic Aspects of the Corrosion Mechanism Applied to Steels. *Electrochem. Impedance Spectrosc.* **2020**, *27*, 137–144. [[CrossRef](#)]
27. Merachtsaki, D.; Xidas, P.; Giannakoudakis, P.; Triantafyllidis, K.; Spathis, P.; Merachtsaki, D.; Xidas, P.; Giannakoudakis, P.; Triantafyllidis, K.; Spathis, P. Corrosion Protection of Steel by Epoxy-Organoclay Nanocomposite Coatings. *Coatings* **2017**, *7*, 84. [[CrossRef](#)]
28. Yang, F.; Yan, D.; Tang, F.; Chen, G.; Liu, Y.; Chen, S. Effect of Sintering Temperature on the Microstructure, Corrosion Resistance and Crack Susceptibility of Chemically Reactive Enamel (CRE) Coating. *Constr. Build. Mater.* **2020**, *238*, 117720. [[CrossRef](#)]
29. Gong, K.; Wu, M.; Xie, F.; Liu, G.; Sun, D. Effect of Dry/Wet Ratio and PH on the Stress Corrosion Cracking Behavior of Rusted X100 Steel in an Alternating Dry/Wet Environment. *Constr. Build. Mater.* **2020**, *260*, 120478. [[CrossRef](#)]
30. Freire, L.; Carmezim, M.J.; Ferreira, M.G.S.; Montemor, M.F. The Electrochemical Behaviour of Stainless Steel AISI 304 in Alkaline Solutions with Different PH in the Presence of Chlorides. *Electrochim. Acta* **2011**, *56*, 5280–5289. [[CrossRef](#)]
31. Ziadi, I.; Akrouf, H.; Hassairi, H.; El-Bassi, L.; Bousselmi, L. Investigating the Biocorrosion Mechanism of 304L Stainless Steel in Raw and Treated Urban Wastewaters. *Eng. Fail. Anal.* **2019**, *101*, 342–356. [[CrossRef](#)]
32. Maocheng, Y.A.N.; Jin, X.U.; Libao, Y.U.; Tangqing, W.U.; Cheng, S.U.N.; Wei, K.E. EIS Analysis on Stress Corrosion Initiation of Pipeline Steel under Disbonded Coating in Near-Neutral PH Simulated Soil Electrolyte. *Corros. Sci.* **2016**, *110*, 23–34. [[CrossRef](#)]
33. Tsouli, S.; Lekatou, A.G.; Nikolaidis, C.; Kleftakis, S. Corrosion and Tensile Behavior of 316L Stainless Steel Concrete Reinforcement in Harsh Environments Containing a Corrosion Inhibitor. *Procedia Struct. Integr.* **2019**, *17*, 268–275. [[CrossRef](#)]